

UNIVERSIDAD SAN FRANCISCO DE QUITO USFQ

Colegio de Ciencias e Ingeniería

**Simulation of a Fluidized bed hydrodynamics using Comsol
Multiphysics**
Trabajo de investigación

Francisco Javier Checa Vaca

Ingeniería Mecánica

Trabajo de titulación presentado como requisito
para la obtención del título de Ingeniero Mecánico

Quito, 23 de diciembre de 2016

UNIVERSIDAD SAN FRANCISCO DE QUITO USFQ
COLEGIO DE CIENCIAS E INGENIERÍA

HOJA DE CALIFICACIÓN
DE TRABAJO DE TITULACIÓN

Simulation of a Fluidized bed Hydrodynamics using Comsol Multiphysics

Francisco Javier Checa Vaca

Calificación:

Nombre del profesor, Título académico

David Escudero, PhD

Firma del profesor

Quito, 23 de diciembre de 2016

Derechos de Autor

Por medio del presente documento certifico que he leído todas las Políticas y Manuales de la Universidad San Francisco de Quito USFQ, incluyendo la Política de Propiedad Intelectual USFQ, y estoy de acuerdo con su contenido, por lo que los derechos de propiedad intelectual del presente trabajo quedan sujetos a lo dispuesto en esas Políticas.

Asimismo, autorizo a la USFQ para que realice la digitalización y publicación de este trabajo en el repositorio virtual, de conformidad a lo dispuesto en el Art. 144 de la Ley Orgánica de Educación Superior.

Firma del estudiante: _____

Nombres y apellidos: Francisco Javier Checa Vaca

Código: 00108478

Cédula de Identidad: 1721233359

Lugar y fecha: Quito, 23 de diciembre de 2016

Resumen

Este estudio presenta simulaciones hidrodinámicas CFD de partículas del grupo Geldart A en un lecho fluidizado utilizando dos tipos de partículas. La simulación se llevó a cabo usando Comsol Multiphysics para flujo multi-fásico, en una configuración de 2 dimensiones (2-D). Se utilizó el enfoque Euler-Euler para simular el comportamiento hidrodinámico del lecho fluidizado. El modelo de viscosidad del tipo Krieger, el modelo de sólidos de presión Gidaspow-Ettehadié y el modelo de arrastre Gidaspow fueron empleados con la condición de slip en la condición de borde para la fase dispersa en la pared, entonces la componente de la velocidad normal a las paredes será cero. Partículas de FCC y partículas de carbón activado fueron simuladas a distintas velocidades de entrada del gas. Las distribuciones de gas-sólido fueron obtenidas con perfiles de velocidad en fase continua como función del tiempo. Una comparación con resultados experimentales fue hecha. Los resultados indican que los lechos fluidizados tienen un comportamiento similar en las simulaciones comparado con los resultados experimentales, comprobando que las simulaciones predijeron correctamente el comportamiento hidrodinámico del lecho fluidizado. Cuando la velocidad de entrada del gas se incrementa, la altura del lecho se incrementa y la concentración de sólidos disminuye.

Key Words: Simulación, CFD, lecho fluidizado, Geldart A

Abstract

This study presents CFD hydrodynamic simulations of Geldart A group particles in a fluidized bed using two different types of particles. The simulation was performed using Comsol Multiphysics for multiphase flow, in a 2 dimensional (2-D) configuration. The Eulerian-Eulerian approach was used to simulate the hydrodynamic behavior of the fluidized bed. Krieger type viscous model, Gidaspow-Ettehadieh solid pressure model and Gidaspow drag model were employed along with slip in the dispersed phase boundary condition for the wall, so the velocity component normal to the wall will be zero. FCC particles and activated carbon particles were simulated with different gas velocities. Gas-solid distributions were obtained along with continuous phase velocity profiles as a function of time. A comparison with experimental results was also done. Results show that the fluidized beds have a similar behavior in the simulation compared to the experimental results, meaning that the simulations predicted successfully the hydrodynamic behavior of the fluidized bed. As the gas velocity increased, the bed height increased and solid concentration inside the bed decreased.

Key Words: Simulation, CFD, fluidized bed, Geldart A

Table of Contents

Introduction	7
Simulation Method	12
Governing Equations	12
Boundary Conditions.....	14
Mesh and Simulation setup.....	15
Results and Discussions	17
Qualitative results	17
Quantitative results.....	22
Comparison with experimental results	25
Conclusions	27
References	29

List of Tables

Table 1. Simulation parameters	16
Table 2. Model parameters for different particles	16

List of Figures

Figure 1. Dimensions of the simulated fluidized bed based on the experimental setup	16
Figure 2. Solids Volume fraction of the FCC particles ($U_g=4\text{cm/s}$) as a function of time	17
Figure 3. Solids Volume fraction of the activated carbon as a function of time for different gas inlet velocities (a) $U_g=4\text{ cm/s}$ (b) $U_g=6\text{ cm/s}$ (c) $U_g=10\text{ cm/s}$	18
Figure 4. Gas velocity (m/s) of the FCC particles as a function of time	20
Figure 5. Gas velocity (m/s) of the activated carbon as a function of time for different gas inlet velocities (a) $U_g=4\text{ cm/s}$ (b) $U_g=6\text{ cm/s}$ (c) $U_g=10\text{ cm/s}$	21
Figure 6. Solid Concentrations measured at a height of 10 cm for: (a) FCC (b) Activated carbon ($U_g=4\text{cm/s}$) (c) Activated carbon ($U_g=6\text{cm/s}$) (d) Activated Carbon ($U_g=10\text{cm/s}$)	23
Figure 7. Solid Concentrations measured at 10 seconds for: (a) FCC (b) Activated carbon ($U_g=4\text{cm/s}$) (c) Activated carbon ($U_g=6\text{cm/s}$) (d) Activated Carbon ($U_g=10\text{cm/s}$)	24
Figure 8. Axial solids velocity in the Y direction at different heights for: (a) FCC (b) Activated carbon ($U_g=4\text{cm/s}$) (c) Activated carbon ($U_g=6\text{cm/s}$) (d) Activated Carbon ($U_g=10\text{cm/s}$)	25
Figure 9. Gas concentrations comparison for: (a) experimental (b) simulated FCC (c) simulated activated carbon (d) Experimental distribution	26

Introduction

A fluidized bed is a multiphase mixture of solid particles and a fluid (liquid or gas) where fluidization takes place when a pressurized fluid passes through the medium of solid particles. Fluidized beds have wide applications in industrial processes in chemical and pharmaceutical industries. Fluidized beds have the advantage of superior heat and mass transfer, better gas-solid contact, operational flexibility and high efficiencies, among their common applications are, coatings onto solids (pills), oil refinery plants, MTO reactors, and some other applications. The study of the hydrodynamic behavior of a fluidized bed will help to improve the reactor performance, maximizing the throughput (Chang, Zhao, Zhang, & Gao, 2016) and will enhance its industrial applications. To start understanding the hydrodynamic behavior of the fluidized bed, the parameter of the minimum fluidization velocity has a big importance in the study of fluidized beds. This velocity marks the start point of fluidization, that is when the drag forces are equal to the particle's weight, and allows the particles to suspend in the gas medium. This parameter depends on the particle type and properties (Escudero, 2014).

To understand the fluidization capabilities of the particles, Geldart classified particles in 4 groups: A, B, C and D. It showed that particles that landed in group A with low density ($<1400 \text{ kg/m}^3$) and low particle diameter, fluidize easily with no bubbling after the minimum fluidization velocity is reached. Particles in group B ($1400 < \rho < 4000 \text{ kg/m}^3$) show bubbling at the minimum fluidization velocity (Pazmiño, 2016). Particles in group C are difficult to fluidize, and in group D with large particle diameter and density can form spouted beds (Geldart, 1973). The particles analyzed in this study are from Geldart A group, in this type of particles, the gas-solid fluidization can be divided

in two regimes, homogenous fluidization and bubbling fluidization. The noticeable characteristic of Geldart A particles are the homogenous fluidization that shows uniform distribution of the particles in the gas phase with no bubbling or agglomerates. This occurs in the interval between the minimum fluidization velocity and minimum bubbling velocity (Sande & Ray, 2014). When the minimum bubbling velocity is reached, it changes the regime from fluidization to bubbling in the fluidized bed. The homogenous fluidization regime is attractive when uniform conditions are needed because it can avoid the solid-phase dead zones, and the particles can be used efficiently (Sande & Ray, 2014).

To understand the complex hydrodynamics of fluidized beds, there are computational fluid dynamics (CFD) models that solve for multiphase flow, but there are specifically two, that are the most used to simulate this type of flow: the Euler-Euler (E-E) approach and the Euler-Lagrange (E-L) approach. The Euler-Lagrange approach treats the gas phase as a continuous phase, defined by an averaged Navier-Stokes equation on a computational cell scale, while the solid phase is treated as a discrete particle, on a single particle scale described by motion law that Newton proposed. This means that this model allows to study the behavior of an individual particle and the interactions between other particles directly, but its biggest disadvantage is that it demands huge computational resources (Zhao, Lu, & Zhong, 2013), so in a large scale systems, there will be difficulties to obtain results in a short period of time, so it is suitable for small domains (Sande & Ray, 2014). Other disadvantage is that the solids pressure and viscosity is neglected, resulting in random motion of the particles during their interaction. This method is applied in some cases when the solid is dilute enough (Peng, Zhu, & Zhang, 2010). In the Euler-Euler approach, it treats both gas and solid

phases as fully inter-penetrating continua (Vashisth, Motlagh, Tebianian, Salcudean, & Grace, 2015) and are described with separate equations of conservations of mass and momentum. The Euler-Euler approach does not have a particle number limit, so it is suitable for large domains, like industrially scale systems, but it requires additional closure equations to describe the solid phase. The drag model of the particles is crucial in this approach to obtain reasonable results (Vashisth et al., 2015).

There are previous studies about simulations of fluidized bed, using both E-E and E-L approaches, and for different cases, particle types and fluidized bed types. A simulation of a turbulent fluidized bed (TBD) carried on Geldart A and B particles, showed that the numerical methods employed to simulate the turbulent fluidized bed were correct, comparing with experimental results. It predicted effectively the hydrodynamic behavior of the TBD on Geldart A and B particles, and showed that there was not a big difference on both types of particles. E-E approach was used in Fluent software to carry out the simulations. The results also showed that the concentrations on the wall are higher than in the center region, and it decreases with the increase of the fluidized bed diameter (Chen, Li, Lv, & Zhu, 2015). Other study simulated fluidized beds on 2-D and 3-D configurations, and compared them to experimental results. E-L approach was used on Geldart A particles on Fluent software, and results showed that the 3-D simulations were successfully resolved, while the 2-D simulations had trouble predicting the particle volume fraction near the wall (Vashisth et al., 2015). A simulation on an industrial turbulent fluidized bed using FCC particles, indicated that the particles tend to ascend in the center of the bed, and descend near to the wall; E-E approach was also employed. The appearance of some vortex flow in the bottom created non-uniform particle velocity and concentrations (Chang et al.,

2016). The importance of the mesh size on simulations of fluidized bed is remarked in these studies, but there is a specific investigation on the meshing importance in simulating fluidized beds. Sande and Ray simulated particles under different mesh sizes, and compared them also with experimental results, to make sure they were correct either improving the quality of the results, or just not. The results showed that mesh refining made the minimum bubbling velocity approach to its experimental value, but reducing its size made no improvement to capture homogenous expansion. Drag models have also a big impact in the E-E approach to predict the hydrodynamic behavior correctly (Sande & Ray, 2014).

The objective of this study is to determine successfully the computational fluid dynamics models that adapt to the experimental results obtained, and to analyze the concentrations of gas-solid in the fluidized bed under different operating conditions (different particles and gas inlet velocities). Two types of particles were used in the experiment and the simulation, both with their own properties like density, viscosity, among other properties. The employed particles are FCC (Fluid Catalytic Cracking) particles and activated carbon particles used on surface coating processes on metals. Both particles land on Geldart A group ($< 1400 \text{ kg/m}^3$) with a low particle diameter and density. Different gas velocities were also applied to reach a steady state of the fluidization.

Simulation Method

Governing Equations

To simulate multiphase flow the Euler-Euler approach was used. This model is present in Comsol Multiphysics 5.2 that solves two sets of Navier-Stokes equations, one set

per phase. The phases interchange momentum as described by the drag model chosen. The volume fraction of the solids is tracked by a transport equation and the pressure is calculated by a mixture-averaged continuity equation (Comsol, 2013).

The governing equations start with the conservation of mass equations. The mass transfer is assumed to be zero between the two phases. The following equations stand for the continuous and dispersed phases(Comsol, 2013):

$$\frac{\partial}{\partial t}(\rho_c \phi_c) + \nabla \cdot (\rho_c \phi_c \mathbf{u}_c) = 0 \quad (1)$$

$$\frac{\partial}{\partial t}(\rho_d \phi_d) + \nabla \cdot (\rho_d \phi_d \mathbf{u}_d) = 0 \quad (2)$$

With the constraint:

$$\phi_c = 1 - \phi_d \quad (3)$$

The continuity equation for the mixture assuming that both phases are incompressible:

$$\nabla \cdot (\phi_d \mathbf{u}_d + \mathbf{u}_c(1 - \phi_d)) = 0 \quad (4)$$

The momentum equations for the continuous and dispersed phase are(Comsol, 2013):

$$\rho_c \phi_c \left[\frac{\partial}{\partial t}(\mathbf{u}_c) + \mathbf{u}_c \nabla \cdot (\mathbf{u}_c) \right] = -\phi_c \nabla p + \nabla \cdot (\phi_c \boldsymbol{\tau}_c) + \phi_c \rho_c \mathbf{g} + \mathbf{F}_{m,c} + \phi_c \mathbf{F}_c \quad (5)$$

$$\rho_d \phi_d \left[\frac{\partial}{\partial t}(\mathbf{u}_d) + \mathbf{u}_d \nabla \cdot (\mathbf{u}_d) \right] = -\phi_d \nabla p + \nabla \cdot (\phi_d \boldsymbol{\tau}_d) + \phi_d \rho_d \mathbf{g} + \mathbf{F}_{m,d} + \phi_d \mathbf{F}_d \quad (6)$$

It's assumed that the fluid phases are Newtonian, so the viscous stress tensors equations are:

$$\boldsymbol{\tau}_c = \mu_c \left(\nabla \mathbf{u}_c + (\nabla \mathbf{u}_c)^T - \frac{2}{3} (\nabla \cdot \mathbf{u}_c) \mathbf{I} \right) \quad (7)$$

$$\tau_d = \mu_d \left(\nabla \mathbf{u}_d + (\nabla \mathbf{u}_d)^T - \frac{2}{3} (\nabla \cdot \mathbf{u}_d) \mathbf{I} \right) \quad (8)$$

For the mixture viscosity is used the Krieger type model, that covers the entire range of particle concentrations(Comsol, 2013):

$$\mu_{mix} = \mu_c \left(1 - \frac{\phi_d}{\phi_{d,max}} \right)^{-2.5\phi_{d,max}} \quad (9)$$

Assume the momentum transfer to be dominated by the drag force, the equation for the drag force is(Griesmer, 2014):

$$\mathbf{F}_{drag,c} = -\mathbf{F}_{drag,d} = \beta \mathbf{u}_{slip} \quad (10)$$

The slip velocity is defined by:

$$\mathbf{u}_{slip} = \mathbf{u}_d - \mathbf{u}_c \quad (11)$$

The Gidaspow drag model is used, so the drag coefficients are defined by(Griesmer, 2014):

$$\beta = \begin{cases} \frac{3\phi_c\phi_d\rho_c C_{drag}}{4d_d} |\mathbf{u}_{slip}| \phi_c^{-2.65} & \text{For } \phi_c > 0.8 \\ 150 \frac{\mu_c \phi_d^2}{\phi_c d_d^2} + 1.75 \frac{\phi_d \rho_c}{d_d} |\mathbf{u}_{slip}| & \text{For } \phi_c < 0.8 \end{cases} \quad (12)$$

The Gidaspow-Ettechadieh pressure model is used:

$$\nabla p_s = -10^{-8.76\phi_c + 5.43} \nabla \phi_c \quad (13)$$

Boundary Conditions

Boundary conditions at the inlet, walls and outlet are needed to be specified to carry out the simulations. Gravitational acceleration is set to all the domains. To avoid

discontinuities at the start and end of the packed bed, a rectangle function is used to define the packed bed column (Griesmer, 2014).

Boundary conditions at the inlet

At the inlet, is a continuous phase inlet type, so that there is just gas entering the fluidized bed. The gas bottom inlet velocity is set for the Y direction and is coupled with a step function that will ramp up the bottom inlet velocity from zero to its full value.

Boundary conditions at the wall

For the dispersed phase velocity boundary condition at the wall, it is set to slip, so the velocity component normal to the wall is zero.

Boundary conditions at the outlet

The mixture boundary condition is set to pressure normal flow.

Mesh and Simulation setup

To simulate, a two-dimensional configuration was enough to simulate the multi-phase flow, because a study showed that the difference between a 2 dimensional model and an axysimetrical model is very small (Peng et al., 2010). The mesh for all the domains where generated by Comsol Multiphysics, the sequence type was a physics controlled mesh with an extremely fine element size. The complete mesh consist of 197776 elements. A quad grid is used near the wall.

Table 1. Simulation parameters

Multiphase flow type	Laminar
Viscosity model	Krieger type
Drag Model	Gidaspow
Solid pressure model	Gidaspow-Ettechadieh
Gas density	1.2 kg/m ³
Gas viscosity	1.8E-5 Pa.s

Table 2. Model parameters for different particles

Particles	FCC	Activated Carbon
Particle density	930 kg/m ³	475 kg/m ³
Particle diameter	54 μm	149 μm
Inlet Gas velocity	4 m/s	4 m/s, 6 m/s, 10 m/s
Solids Volume Fraction	0.60	0.64



Figure 1. Dimensions of the simulated fluidized bed based on the experimental setup

Results and Discussions

The results were classified on qualitative and quantitative, to obtain more precise data. After this, a comparison with experimental data is also made. For the qualitative results, two types of snapshots were obtained, for the gas velocity continuous phase, and the dispersed phase concentration (solid concentrations), for different simulation times.

Qualitative results

The results of simulations showed a similar hydrodynamic behavior, with the behavior previously analyzed by (Zhang, Zhang, & Zhang, 2003), there is a circulation of solid particles that follow certain patterns. Zhang et al. showed that the gas tried to ascend by the center of the bed, carrying particles and leaving them on the top of the fluidized bed. They named the center region as jetting region. Then, a downward flow is created near the wall that carries the particles that are in the top of the bed, finally there is recirculation zone, the particles reach the bottom, and ascend again on the top.

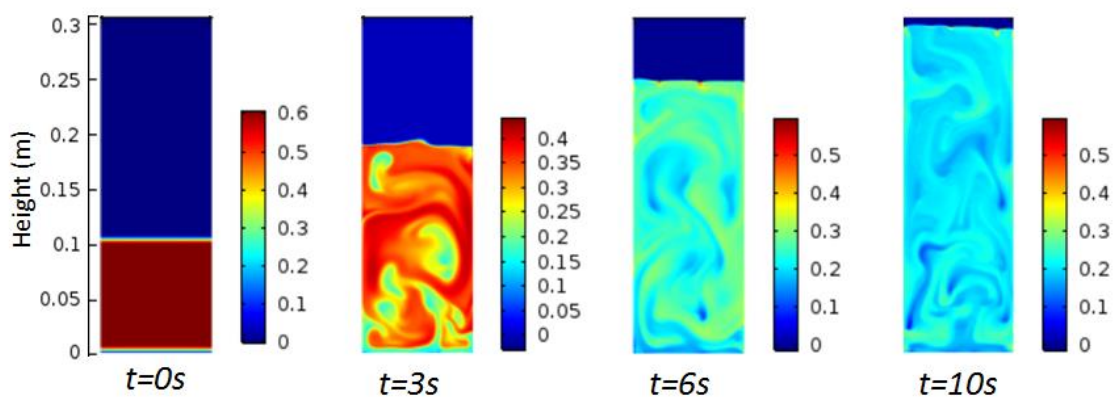


Figure 2. Solids Volume fraction of the FCC particles ($U_g=4\text{cm/s}$) as a function of time

As you can see from Figure 2. Solids Volume fraction of the FCC particles ($U_g=4\text{cm/s}$) as a function of time, the FCC particles follow a similar pattern, even though there are a lot

of patterns specially at 10 seconds, but looking at the voids that are formed between the walls and the center region, the solids have a downward flow near the wall. The simulations carried on activated carbon particles (Figure 3) show this pattern better.

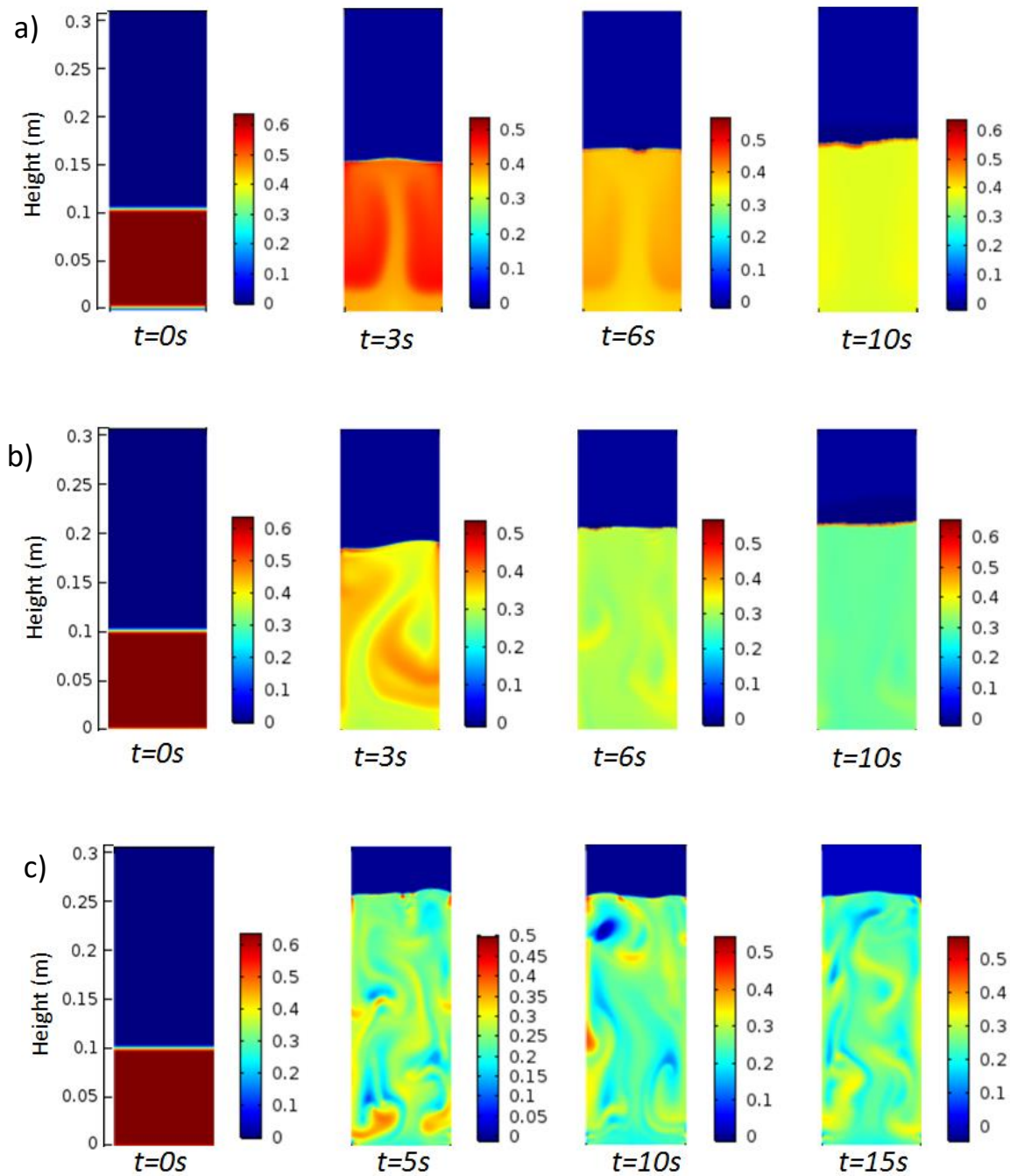


Figure 3. Solids Volume fraction of the activated carbon as a function of time for different gas inlet velocities (a) $U_g=4$ cm/s (b) $U_g=6$ cm/s (c) $U_g=10$ cm/s

The activated carbon particles also showed a behavior similar to the FCC particles, especially when the gas velocity is 10 m/s, as we can see from Figure 3. Solids Volume fraction of the activated carbon as a function of time for different gas inlet velocities (a) $U_g=4$ cm/s (b) $U_g=6$ cm/s (c) $U_g=10$ cm/s, there is a pattern that these particles also follow, an upward flow carry particles to the top, then particles circulate downward near the wall. The (a) and (b) cases in the same figure show a more clear shape, with not much voids formed. The path is defined when the time is between 3 and 6 seconds, the solids concentrations is less in the center due to the upward flow. After this time, the fluidized bed enters a state where there is not much change in solid concentration or bed height, reaches a steady state. For the c) case, it was simulated until 15 seconds, and it show a more chaotic behavior, similar to the 10 seconds for the FCC particles. The difference is the heaviness of the particles, the activated carbon are almost 3 times bigger the particle diameter, meaning that those particles are heavier, that is why the results show that to reach a similar result needs a higher gas velocity, even at 10 m/s, the bed height is at 25 cm compared to the almost 30 cm on the FCC particles. The differences between the fluidization of both particles can be seen clearly comparing Figure 3. Solids Volume fraction of the activated carbon as a function of time for different gas inlet velocities (a) $U_g=4$ cm/s (b) $U_g=6$ cm/s (c) $U_g=10$ cm/s and Figure 2. Solids Volume fraction of the FCC particles ($U_g=4$ cm/s) as a function of time FCC particles show higher solid concentrations at early time, but have lower concentrations at 10 seconds, comparing to the activated carbon.

The other hydrodynamic behavior that the particles show when they are in fluidization, the bed height starts to increase, depending on the gas velocity, and the solid concentration decrease. The concentration of the particles in the Figure 3. Solids

Volume fraction of the activated carbon as a function of time for different gas inlet velocities (a) $U_g=4$ cm/s (b) $U_g=6$ cm/s (c) $U_g=10$ cm/s, for case (a) show that at 10 seconds the solid concentration on most of the bed is 0.4, for the case (b) is at 0.3 and for the (c) case is between 0.3 and 0.2, due to the not uniform solids concentrations. There are zones with low fluidization, where the solid is more concentrated in the figures, these low fluidization regions are located especially between the wall and the center of the bed. Voids are also formed in these zones.

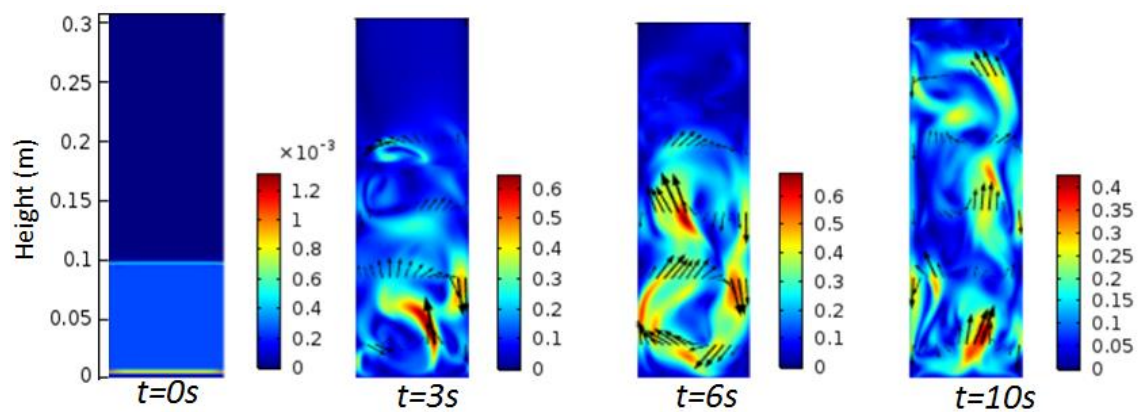


Figure 4. Gas velocity (m/s) of the FCC particles as a function of time

The velocity profiles of the Figure 4. Gas velocity (m/s) of the FCC particles as a function of time show the velocity vectors that the gas has at that instant. The hydrodynamic behavior of recirculation in the fluidized bed can be proved looking at the vectors direction. The vectors point upward near the center of the bed, and are larger, so the velocity is higher in that position. The vectors near the wall show a downward flow, meaning that the particles are descending near the wall.

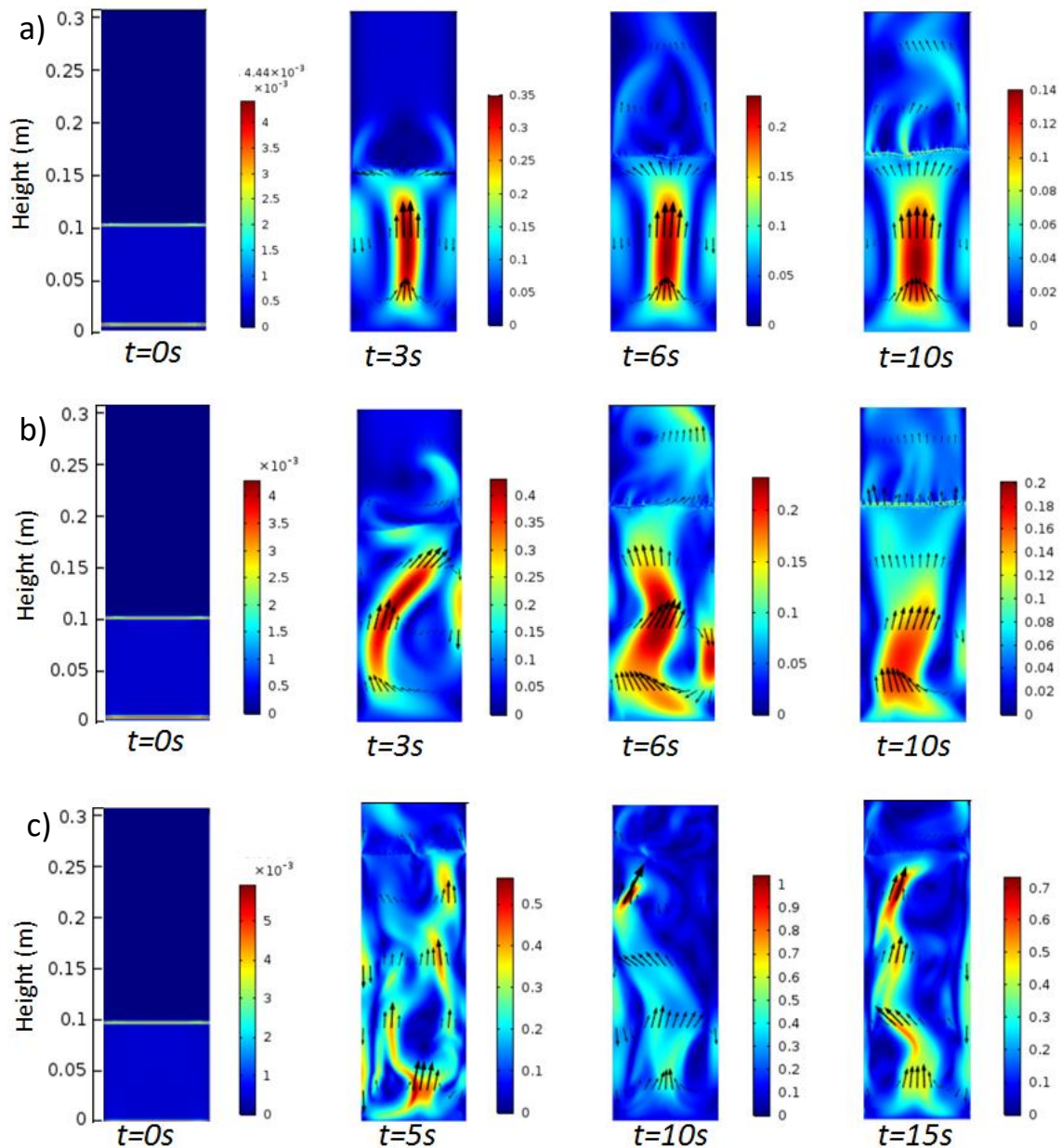


Figure 5. Gas velocity (m/s) of the activated carbon as a function of time for different gas inlet velocities (a) $U_g = 4$ cm/s (b) $U_g = 6$ cm/s (c) $U_g = 10$ cm/s

The vectors for the velocity profiles of Figure 5. Gas velocity (m/s) of the activated carbon as a function of time for different gas inlet velocities (a) $U_g = 4$ cm/s (b) $U_g = 6$ cm/s (c) $U_g = 10$ cm/s show the same behavior previously explained, especially for the cases (a) and (b), the path of the gas velocity is clearly described in the center, the vectors point upward and the velocity is higher, comparing to the wall, where the vector point downward but are smaller, so the velocity is lower but follows the re-circulation pattern. These figures

help to understand where the voids and the low fluidization is, in the parts of the bed where there is almost no gas velocity (blue), means that there is a higher solid concentration that has a low fluidization or is not fluidized, and are called dead zones.

Quantitative results

The qualitative results were obtained for different conditions, to get a better view of the particle distribution at different heights and times. Velocity plots were also obtained. The Figure 6. Solid Concentrations measured at a height of 10 cm for: (a) FCC (b) Activated carbon ($U_g=4\text{cm/s}$) (c) Activated carbon ($U_g=6\text{cm/s}$) (d) Activated Carbon ($U_g=10\text{cm/s}$) is a set of plots measured at a height of 10 cm. The (a) case show the fluidization of the FCC particles, and it show the solid concentrations on the sides, while there are zones between the wall and the center that show lower solid concentrations, and is where the gas is flowing. The peaks of concentration may be low fluidization zones. In the activated carbon particles, in case (b) since there is low gas velocity, the fluidized bed reaches a steady state faster than the other cases, that's why the curve for 6 and 10 seconds is similar. The low solid concentrations mean that the gas is flowing there, so the solids concentrations will decrease. For the cases (c) and (d), that have higher gas inlet velocities, the solid concentrations behavior is similar, there is a higher concentrations on the sides, near the walls, and in the center, compared to the zones in between them. The particles flowing upward and downward are the reason of those concentrations, but in the low concentration zones is where the gas is flowing.

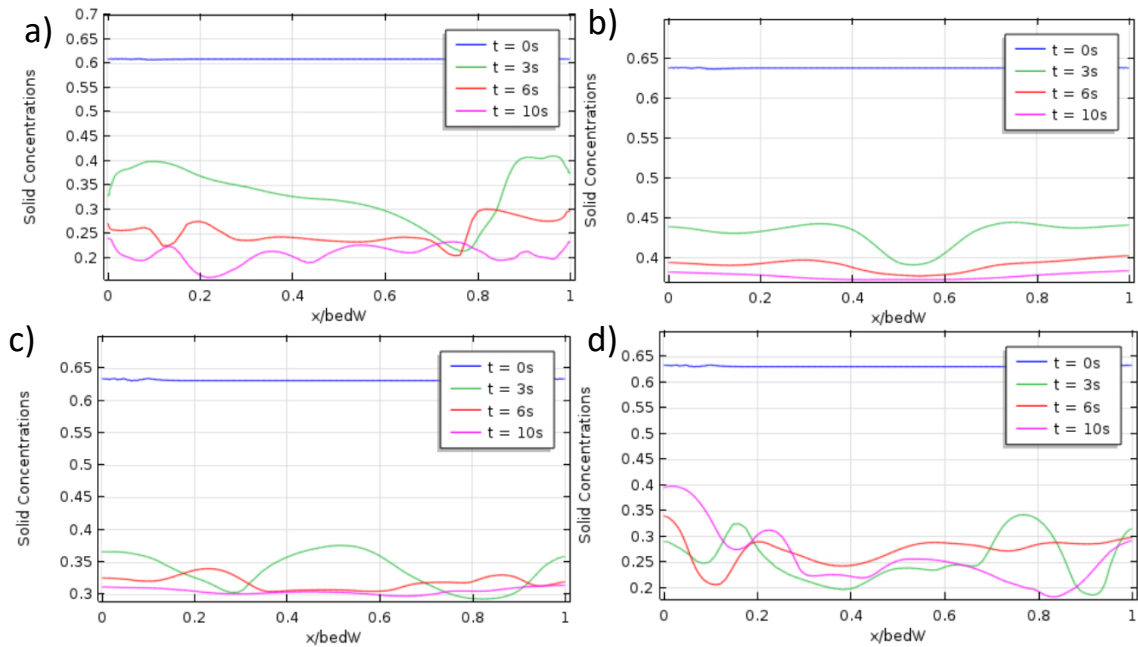


Figure 6. Solid Concentrations measured at a height of 10 cm for: (a) FCC (b) Activated carbon ($U_g=4\text{cm/s}$) (c) Activated carbon ($U_g=6\text{cm/s}$) (d) Activated Carbon ($U_g=10\text{cm/s}$)

The Figure 7. Solid Concentrations measured at 10 seconds for: (a) FCC (b) Activated carbon ($U_g=4\text{cm/s}$) (c) Activated carbon ($U_g=6\text{cm/s}$) (d) Activated Carbon ($U_g=10\text{cm/s}$) is analyzed at the same time of fluidization, 10 seconds in all the cases and at the same heights too. In the (a) case, for FCC, the behavior is chaotic, similar to the (d) case, there is variation of the concentrations that tend to follow the same direction except for the one in the 2.5 cm height, that has the lowest concentration, that means that there is a lot of gas flowing in that position. The (b) case show an uniform curve, and all are similar, for the top and bottom curves have similar values. This case show that the gas is just trying to flow upward in the center, with not much particle carrying, at that velocity, the gas does not have too much force compared to the other cases. For the (c) and (d) cases, there is a certain pattern that the curves have, even though the curves are not uniform, they follow a “U” path, higher solid concentrations on the sides, lower solid concentrations on the center. The gas is flowing upward and faster in the center, so there is more fluidization there compared to the flow near the walls, where particles

flow downward and slower. To analyze the dead zones it will be better to see them in the velocity plots.

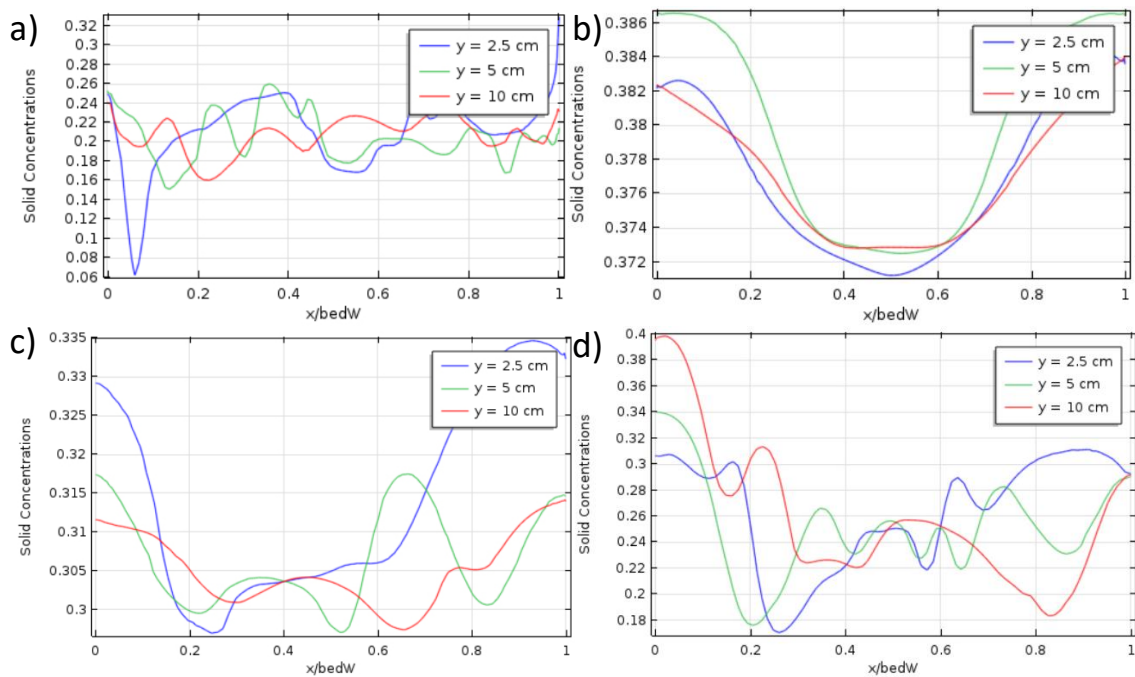


Figure 7. Solid Concentrations measured at 10 seconds for: (a) FCC (b) Activated carbon ($U_g=4\text{cm/s}$) (c) Activated carbon ($U_g=6\text{cm/s}$) (d) Activated Carbon ($U_g=10\text{cm/s}$)

For the velocity of the solids, the Figure 8. Axial solids velocity in the Y direction at different heights for: (a) FCC (b) Activated carbon ($U_g=4\text{cm/s}$) (c) Activated carbon ($U_g=6\text{cm/s}$) (d) Activated Carbon ($U_g=10\text{cm/s}$) have the dispersed phase velocity plots measured at 10 seconds in all the cases, for the y component of the velocity at different heights. All the cases show a similar pattern, and the main reason is the re-circulation pattern that the fluidized bed, the upward flow is in the center, and has the highest positive velocities there, due to the direction of the flow. The zones near the wall show negative velocities, this explains the downward flow that carries the particles to the bottom to re-circulate. The velocities that are 0 and near show where the dead zone are, and is where the gas has low velocity.

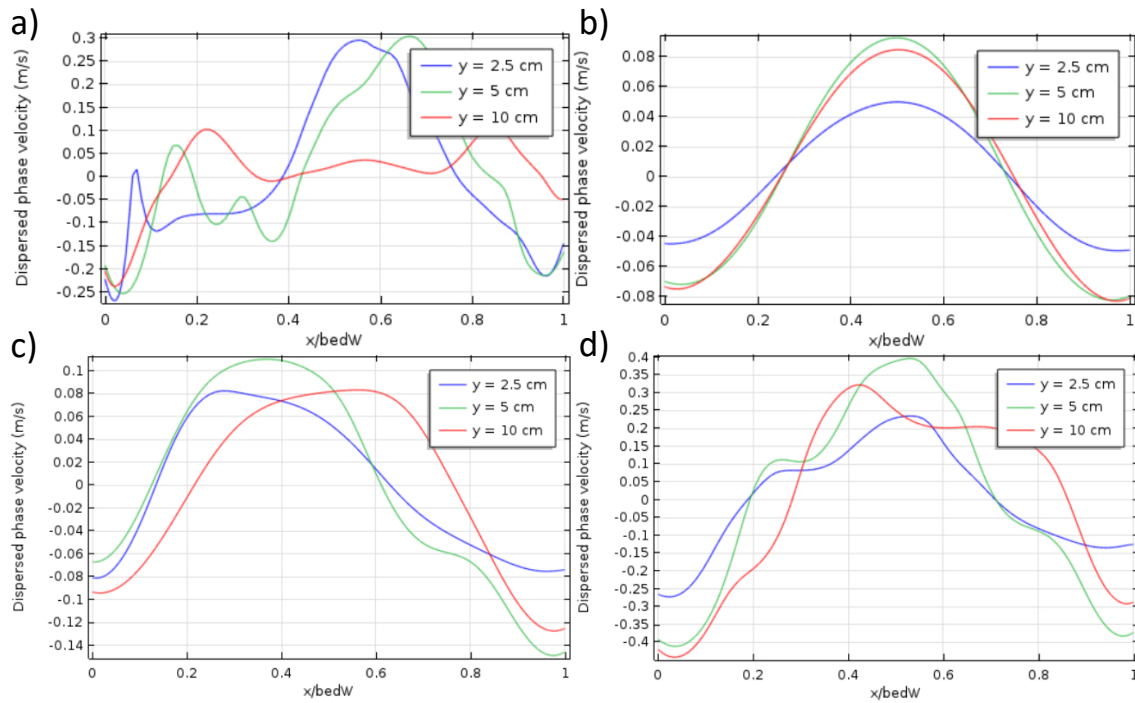
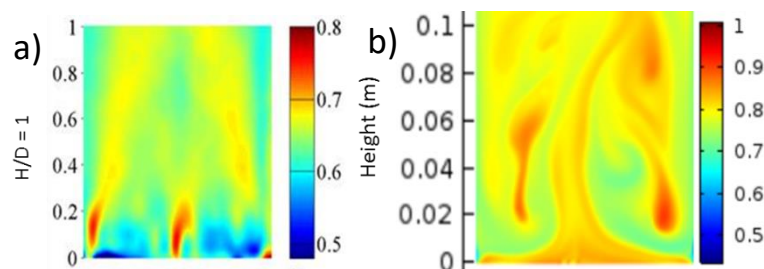


Figure 8. Axial solids velocity in the Y direction at different heights for: (a) FCC (b) Activated carbon ($U_g=4$ cm/s) (c) Activated carbon ($U_g=6$ cm/s) (d) Activated Carbon ($U_g=10$ cm/s)

Comparison with experimental results

The simulation results were compared with the experimental results that David Escudero obtained in his investigations. He built up the fluidized bed with the same dimensions as the ones used in these simulations, and fluidized 2 types of particles, glass beads and walnut shell particles (Escudero, 2014). To compare with this study, the particles analyzed are walnut shell with a solid density of 1440 kg/m^3 and a particle diameter of $212\text{--}425 \text{ }\mu\text{m}$, and the solids height was $H=1D$, the same as this study.



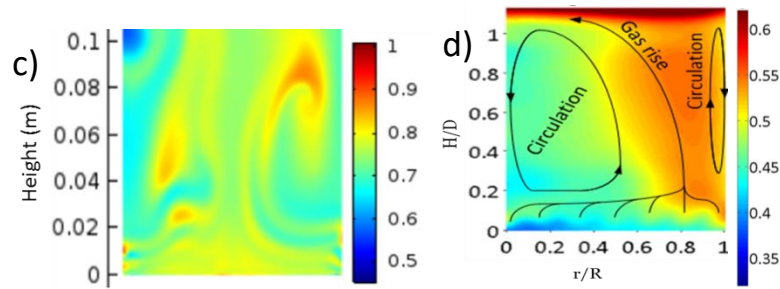


Figure 9. Gas concentrations comparison for: (a) experimental (b) simulated FCC (c) simulated activated carbon (d) Experimental distribution

The comparison made in Figure 9. Gas concentrations comparison for: (a) experimental (b) simulated FCC (c) simulated activated carbon show the gas concentration in all the cases. In the (a) case, the experimental results show a higher concentration of the gas in the center and in the zones between the wall and the center, and compared to the (b) and (c) cases the gas distribution is similar, it has higher concentration in positions that are close to the experimental data. The experimental results show the recirculation pattern, the low gas concentration on the sides is due to the downward flow that is carrying the particles. The quantitative results were also similar, especially to the (d) plot of Figure 6. Solid Concentrations measured at a height of 10 cm for: (a) FCC (b) Activated carbon ($U_g=4\text{cm/s}$) (c) Activated carbon ($U_g=6\text{cm/s}$) (d) Activated Carbon ($U_g=10\text{cm/s}$) at 15 seconds, compared to the plots obtained in the experimental investigation, this validate the results obtained by the simulations. In figure 9 in the last plot (d) the circulation pattern is described for the experimental results, and it shows the circulation zones, similar to the simulations obtained (Drake, 2011). The principal difference is that, the inlet was assumed to be one inlet with the width of the radius of the bed, while in the experiment the inlet has several small entrances, that's why it shows a slightly different pattern in the entrance.

The software that carried the simulations, Comsol Multiphysics 5.2, simulated successfully the particles that were analyzed in this study, but the program has some limitations to simulate fluidized beds. One of the limitations is the limit of the dimensions of the simulated particles, it showed that the software simulated without trouble particles of Geldart A group, while it didn't converged particles of Geldart B, C and D, so the model for laminar flow simulate small and not so heavy particles. Other limitation is the gas inlet velocity; the simulation did not converge at very low gas inlet velocities, but didn't show a limitation at high gas inlet velocities. The most important parameter probably was the meshing of the fluidized bed, because the coarser grids didn't seem to converge any simulation, so while the grid size where decreasing, the convergence increased, until the extremely fine grid that Comsol generated, this may be due to the details that the particles show when fluidized. The program could not generate a finer grid than the used in these simulations, and the simulation time also increased, some simulations took more than a day to end and obtain results. The relative tolerances of all the simulations were of 0.1, except for the simulation of the case of the activated carbon particles at 4cm/s that were 0.2, because it did not converged at a lower relative tolerance.

Conclusions

The software used for the simulations, simulated successfully for two types of particles, the FCC particles and the activated carbon particles, using the Euler-Euler model, the results of solid concentrations and velocities were successfully obtained. While there were convergence problems with the limitations, the results obtained showed a circulation pattern that the particles follow when the fluidized bed is fluidized. The particles are carried to the top of the fluidized bed when the gas enters,

and form an upward flow in the center of the bed. Then the particles fall to the sides near the wall, and are carried to the bottom in a downward flow, where the particles again reach the center and ascend again, forming a re-circulation pattern in the fluidized bed. The pattern is clearly defined in the snapshots of the activated carbon of figure 3 at gas inlet velocities of 4 cm/s and 6cm/s, where there is uniformity along the fluidized bed and a steady state is reached at the end. The other results, activated carbon particles at 10 cm/s and FCC particles show a more chaotic behavior, with not defined concentrations zones or gas paths, but the fluidized particles tend to flow upward in the center or near it, and flow downward at the walls. The dead zones can be identified in the velocity results of Figure 4 and Figure 5, where the gas has low velocity, and also in the dispersed phase velocity plots of Figure 8. The comparison of the experimental results and the simulations showed the similarities in the circulation pattern of the particles, the gas distributions where similar.

Notation

C_{drag} = drag coefficient

d_d = particle diameter (m)

F_{drag} = Drag force (N/m³)

F = Volume force (N/m³)

F_m = interphase momentum transfer (N/m³)

g = gravitational acceleration (m/s²)

I = unit tensor

p = pressure (Pa)

p_s = Solid pressure

u = velocity(m/s)

Greek letters

β = drag coefficient

ρ = density (kg/m³)

\emptyset = volume fraction

τ = stress tensor (Pa)

μ = viscosity (kg/m.s)

Subscripts

c = continuous phase

d = dispersed phase

References

- Chang, J., Zhao, J., Zhang, K., & Gao, J. (2016). Hydrodynamic modeling of an industrial turbulent fluidized bed reactor with FCC particles. *Powder Technology*, 304, 134–142. <http://doi.org/10.1016/j.powtec.2016.04.048>
- Chen, J., Li, H., Lv, X., & Zhu, Q. (2015). A structure-based drag model for the simulation of Geldart A and B particles in turbulent fluidized beds. *Powder Technology*, 274, 112–122. <http://doi.org/10.1016/j.powtec.2015.01.010>
- Comsol. (2013). The CFD Module User's Guide. *Comsol Guide*.
- Drake, J. (2011). Hydrodynamic Characterization of 3D Fluidized Beds Using Noninvasive Techniques.
- Escudero, D. (2014). Characterization of the Hydrodynamic Structure of a 3D Acoustic Fluidized Bed, 53–81.
- Geldart, D. (1973). Types of Gas Fluidization. *Powder Technology*, 285–292.
- Griesmer, A. (2014). Circulating Fluidized Bed. *Comsol Guide*, 1–26.
- Pazmiño, M. (2016). Hydrodynamic Study for a Granular Material Used in Pack

Carburizing Processes in a Cold Fluidized Bed Trabajo experimental Michaelle

Alejandra Pazmiño Pazmiño Michaelle Alejandra Pazmiño Pazmiño, 44.

Peng, B., Zhu, J., & Zhang, C. (2010). Gas - Solids Circulating Fluidized-Bed Risers, 5310–5322.

Sande, P. C., & Ray, S. (2014). Mesh size effect on CFD simulation of gas- fluidized Geldart A particles. *Powder Technology*, 264, 43–53.
<http://doi.org/10.1016/j.powtec.2014.05.019>

Vashisth, S., Motlagh, A. H. A., Tebianian, S., Salcudean, M., & Grace, J. R. (2015). Comparison of numerical approaches to model FCC particles in gas – solid bubbling fluidized bed. *Chemical Engineering Science*, 134, 269–286.
<http://doi.org/10.1016/j.ces.2015.05.001>

Zhang, K., Zhang, J., & Zhang, B. (2003). Experimental and numerical study of fluid dynamic parameters in a jetting fluidized bed of a binary mixture. *Powder Technology*, 132(1), 30–38. [http://doi.org/10.1016/S0032-5910\(03\)00041-X](http://doi.org/10.1016/S0032-5910(03)00041-X)

Zhao, Y., Lu, B., & Zhong, Y. (2013). Euler-Euler modeling of a gas-solid bubbling fluidized bed with kinetic theory of rough particles. *Chemical Engineering Science*, 104, 767–779. <http://doi.org/10.1016/j.ces.2013.10.001>